UC Irvine
UC Irvine Previously Published Works

Authors

Wang, Weihong

Aregahegn, Kifle Z

Andersen, Simone T

et al.

Peer reviewed

Quantum Yields and N_2O Formation from Photolysis of Solid Films of Neonicotinoids

Weihong Wang,[†] Kifle Z. Aregahegn,[†,‡] Simone T. Andersen,[†,§] Anton Z. Ni,[†] Andrea F. Rohrbacher,[†] Ole John Nielsen,[§] and Barbara J. Finlayson-Pitts*,[†]

[†]Department of Chemistry, University of California, Irvine, Irvine, California 92697-2025, United States
[‡]Department of Chemistry, Debre Berhan University, P.O. Box 445, Debre Berhan, Ethiopia
[§]Copenhagen Center for Atmospheric Research, Department of Chemistry, University of Copenhagen, 2100 Copenhagen Ø, Denmark

Ⓢ *Supporting Information*

ABSTRACT: Neonicotinoids (NN), first introduced in 1991, are found on environmental surfaces where they undergo photolytic degradation. Photolysis studies of thin films of NN were performed using two approaches: (1) transmission FTIR, in which solid films of NN and the gas-phase products were analyzed simultaneously, and (2) attenuated-total-reflectance FTIR combined with transmission FTIR, in which solid films of NN and the gas-phase products were probed in the same experiment but not at the same time. Photolysis quantum yields using broadband irradiation centered at 313 nm were $(2.2 \pm 0.9) \times 10^{-3}$ for clothianidin (CLD), $(3.9 \pm 0.3) \times 10^{-3}$ for thiamethoxam (TMX), and $(3.3 \pm 0.5) \times 10^{-3}$ for dinotefuran (DNF), with all errors being ±1s. At 254 nm, which was used to gain insight into the wavelength dependence, quantum yields were in the range of $(0.8-20) \times 10^{-3}$ for all NNs, including acetamiprid (ACM) and thiacloprid (TCD). Nitrous oxide (N_2O), a potent greenhouse gas, was the only gas-phase product detected for the photolysis of nitroguanidines, with yields of $\Delta N_2O/\Delta NN > 0.5$ in air at both 313 and 254 nm. The atmospheric lifetimes with respect to photolysis for CLD, TMX, and DNF, which absorb light in the actinic region, are estimated to be 15, 10, and 11 h, respectively, at a solar zenith angle of 35° and 12, 8, and 10 h at a solar zenith angle of 15°.

KEYWORDS: *neonicotinoids, clothianidin, thiamethoxam, dinotefuran, acetamiprid, thiacloprid*

INTRODUCTION

In 1991, the first neonicotinoid (NN), imidacloprid (IMD), was introduced. In the following years, six more were added: nitenpyram (NPM) and acetamiprid (ACM) in 1995, thiamethoxam (TMX) in 1998, thiacloprid (TCD) in 2000, clothianidin (CLD) in 2001, and dinotefuran (DNF) in 2002.[1−3] The structures of the NNs are shown in Figure 1. NNs bind to nicotine acetylcholine receptors in the target species, primarily sucking insects such as aphids.[1,2,4−7] Although they were thought to have relatively low nontarget toxicity,[8,9] deleterious effects of neonicotinoids are increasingly being reported,[10,11] for example, in birds,[12,13] humans,[5−7,14−19] vertebrates,[20] invertebrates,[21−23] and pollinators (especially bees),[24−47] leading to their recent regulation by the European Union.

Insecticides are dispersed into the environment when applied to soil, foliage and seeds and are also used for flea control on cats and dogs.[4] In the environment, insecticides can undergo hydrolytic, photolytic and microbial degradation,[48] with photolysis being one of the major environmental fates for compounds that absorb in the actinic region above 290 nm. Studies to date have focused mainly on photolysis in aqueous solutions.[49−52] However, Bonmatin et al.[48] reported that mechanical abrasion of seeds during planting contaminates the surrounding land and vegetation surfaces with the NN coating, providing a nonaqueous route of exposure for honeybees.

A few studies have been done on photolysis of solid thin films of imidacloprid[53−56] and nitenpyram.[57] Gaseous nitrous oxide (N_2O), a greenhouse gas with a global-warming potential

of 264 relative to CO_2 on a 20 year scale,[58] was previously identified as the gas-phase product in the photolysis of solid thin films of IMD and NPM.[56,57] The goals of the current study were to determine the N_2O and photolysis quantum yields for thin solid films of five other NNs, CLD, TMX, DNF, ACM, and TCD, using attenuated total reflectance (ATR)-FTIR at 254 nm and at wavelengths in the actinic region for those that absorb above 290 nm. The yields of N_2O were measured using two approaches: transmission through the ATR cell above the crystal after measurement of the solid film or direct transmission in a separate cell through the solid and gas phase simultaneously. Because the latter technique is different from that used previously for IMD and NPM, N_2O yields for these compounds were measured this way as well. Atmospheric lifetimes of the NNs with respect to photolysis were calculated using the measured quantum yields and absorption cross sections, and the relative contribution of the production of N_2O from NN photolysis to the global flux was estimated.

EXPERIMENTAL PROCEDURES

Experiments were performed using two different infrared (IR) cells with a 10 cm path length and volumes of 7.5 or 25 cm^3 (Figure 2). Barium fluoride windows (BaF_2, Edmund Optics or Crystran Limited,
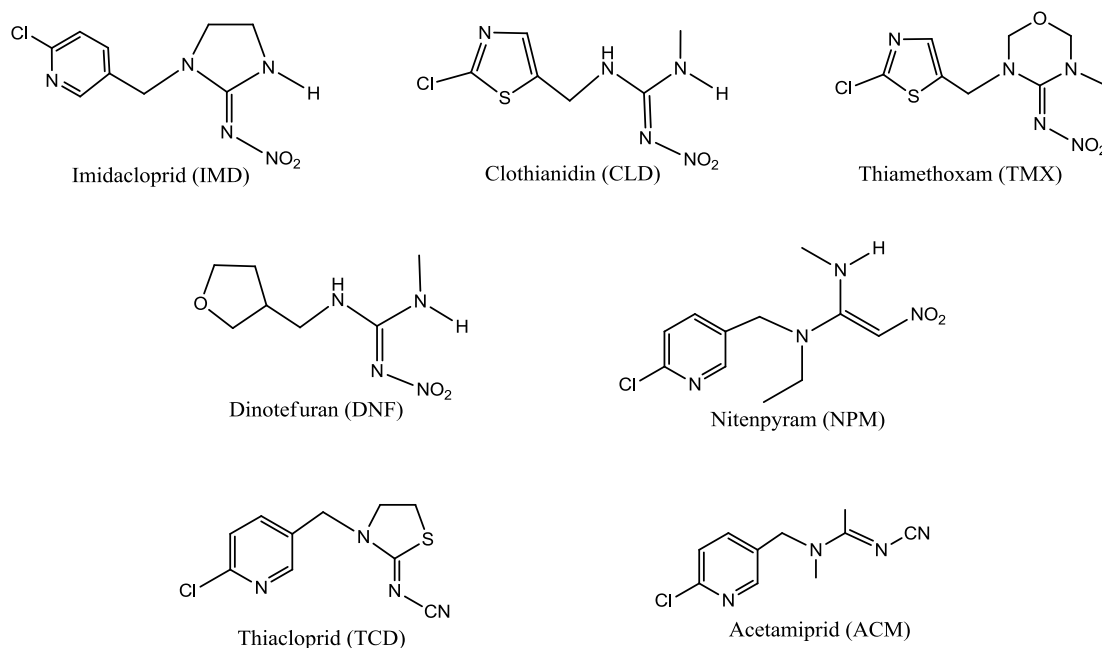
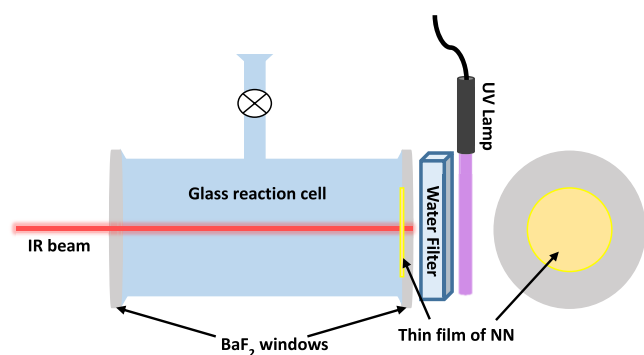**Figure 1.** Structures of neonicotinoids used in this study.

Figure 2. Schematic of transmission-IR cell for the photolysis of neonicotinoids.

25 mm in diameter, 3 mm thick) were used on the cell because of their wide transmission range from the IR through to the ultraviolet (UV) range. The cell was placed in a custom-built holder located in the center of the sampling compartment of an IR spectrometer (Mattson, Cygnus 100, FTIR).

Surface films of the neonicotinoids were formed by applying a small amount of NN in acetonitrile solution (concentration ranged from 2 mg/mL to 6 mg/mL) on a BaF_2 window, leaving a thin film of NN on the window as the solvent evaporated in air. The window was then mounted on the cell with the NN film on the inner surface and irradiated through the BaF_2 window. Two lamps were used: a low-pressure mercury lamp at 254 nm (Jelight, 81-3306-2) and a low-pressure organic-phosphor-coated mercury lamp (Jelight, 84-2061-2) with broadband emission centered around 313 nm; the latter lamp contained some mercury lines and was referred to previously as a 305 nm lamp (see Figure S1 for the spectral distributions of the lamps). Although 254 nm light does not reach the Earth's surface, this provided some insight into wavelength dependencies for the quantum yields and N_2O formation. When the 313 nm lamp was used, a glass water filter (Fisher Brand, optical glass 6030) was placed in between the lamp and the BaF_2 window to remove unwanted light below 290 nm and prevent heating from the longer-wavelength radiation. The photolysis was carried out with the cell under vacuum or in air (Praxair, Ultra Zero grade) or N_2 (Praxair, 99.999%) added to a total pressure of 500−650 Torr. After selected photolysis intervals (typically 1 min for

the 254 nm lamp and 30 min for the 313 nm lamp), the lamp was removed to transmit the IR beam through the cell.

For quantification, it was important to ensure that the IR beam that was detected had passed through the NN film and did not include parts of the window closer to the edges that were not coated. Thus, a mask was used to restrict the IR beam to a smaller rectangular area in the center of the window that always had NN. The fraction of the total NN area on the window that was covered by this rectangular section was estimated. It was then assumed that the fractional NN loss measured in this section applied to the NN on the entire window. This is one of the largest uncertainties in the calculated N_2O yields. Infrared spectra (128 scans, 1 cm^{-1} resolution), which probed both the solid film on the window and the gas phase together, were taken before and after each photolysis interval. The experiments were carried out until there was about a 50% loss of the NN.

Photolysis quantum yields and N_2O yields were also measured using ATR-FTIR. A thin film of NN was formed on the top surface of a Ge ATR crystal. The ATR crystal was then placed in a reaction cell (Figure S2 in the Supporting Information), described in detail elsewhere.[56,57] The NN films were irradiated with the lamps described above. In this experiment, the lamp was warmed up for at least 30 min before initiation of photolysis in order to stabilize the emission intensity. The ATR-FTIR spectra of the NNs were recorded (Mattson, Galaxy 5020, 4 cm^{-1} resolution, 128 scans) before and during irradiation. After the irradiation, the cell was repositioned to direct the IR beam through the cell above the crystal to measure gas-phase products via transmission FTIR. Photolysis quantum yields for NN were measured as the number of molecules of the NN lost per cm^2 per second divided by the number of photons striking the sample per cm^2 per second.

Photoisomerization of 2-nitrobenzaldehyde (2-NB) to 2-nitrosobenzoic acid was used as a chemical actinometer to convert the relative intensities of the lamps to absolute values, as described in earlier studies.[56] The experimental setup had changed somewhat when the CLD measurements were carried out, so that quantum yields for CLD were determined relative to IMD. The errors cited for CLD include the errors in the quantum yields of the reference compound used, IMD.

The advantage of using transmission FTIR is that the solid film and gas phase are probed at the same time, but the photolysis and the solid and gas-phase measurements are carried out in discrete time intervals rather than being continuous. The yields of N_2O were obtained from plots of the number of molecules of N_2O produced versus the number of molecules of NN reacted, $\Delta N_2O/\Delta NN$. The major source of error in determining N_2O yields in the transmission experiments
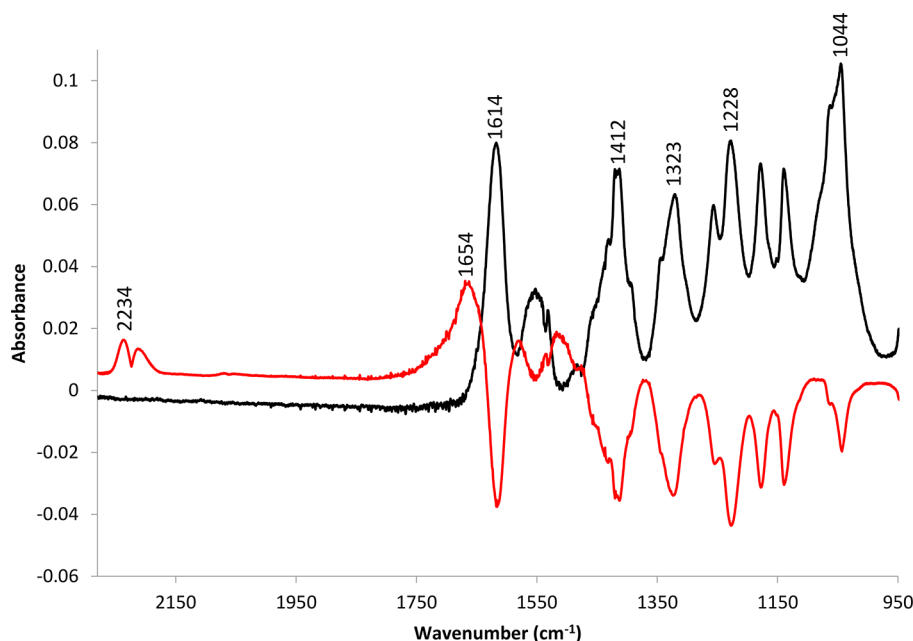
Figure 3. Transmission-FTIR spectrum of CLD before photolysis (black) and the difference spectrum (red) after 17 min of irradiation using the 254 nm lamp. The difference spectrum is $\log(S_1/S_2)$, where S_1 is the single-beam spectrum of CLD before photolysis, and S_2 is the single-beam spectrum after photolysis.

was the uncertainty in obtaining the absolute number of NN lost over the entire sample on the basis of the IR measurements over a smaller portion of the film; uneven film thicknesses, for example, would affect this extrapolation. During the continuous photolysis of the NN thin films using ATR-FTIR, the loss of NN was followed, but the gaseous product, N_2O, could only be measured at the end of the experiment. The major source of uncertainty in this case was that the yields were based on one data point per experiment. Despite these uncertainties, the results using the two approaches were the same within experimental error.

The sources and purities of the neonicotinoids were as follows: IMD (Chem Service, 99.5%), CLD (Chem Service, 99.5%), TMX (Sigma-Aldrich, Pestanal, Analytical Standard), DNF (Chem Service, 99.5%), NPM (Sigma-Aldrich, 99.9%), ACM (Sigma-Aldrich, Pestanal, Analytical Standard), and TCD (Sigma-Aldrich, Pestanal, Analytical Standard). Calibration of the NNs in the infrared were carried out using a liquid transmission cell with path length of 0.143 mm. The solutions were prepared by dissolving NN in acetonitrile (ACN, J. T. Baker, LC/MS grade). The infrared absorbance of the NNs in the ACN solutions at concentrations over the range from 1 to 10 mg/mL were measured. The concentration of NN was then converted to the absolute number of NN molecules, which could be used to determine the number of NN molecules in the thin films, assuming the same absorption coefficients in solution and the thin films. Calibration of N_2O (Matheson, UHP) was done in the same cell used in the experiments from custom mixtures of known concentrations in air from 16 to 600 Torr total pressure. The calibration was constant over this pressure range.

■ RESULTS AND DISCUSSION

All neonicotinoids absorb at 254 nm. However, only the four nitroguanidines and NPM, all of which contain an $-NO_2$ group, absorb out into the actinic region beyond 290 nm[59] (Figure S1; the UV−vis absorption spectra of NPM and IMD were reported earlier by Aregahegn et al.[57]). Table S1 in the Supporting Information shows the absorption cross sections (base 10) for nitroguanidines at 313 nm.

Figure 3 (black line) shows a typical transmission-FTIR spectrum of CLD as an example of a nitroguanidine characterized by a $-C{=}N{-}NO_2$ group. Peaks at 1614 and 1228 cm^{-1} are due

to the asymmetric and symmetric vibrations, respectively, of the $-NO_2$ group.[60] After irradiation, the difference spectrum (red line in Figure 3), shows the loss of CLD and the formation of N_2O (2234 cm^{-1} peak) and a new product with a broad band at ~1654 cm^{-1} due to a $-C{=}O$ and/or $-C{=}N$ group.[60] The absorbance at 1614 cm^{-1} is used to monitor the loss of CLD (see Table S2 for the infrared-absorption cross sections for the peaks used for nitroguanidines and NPM) and the absorbance at 2234 cm^{-1} is used for N_2O formation. Other gas-phase products, such as NO and NO_2, were not observed.

Photolysis Rates and Quantum Yields. Photolysis of the neonicotinoids at 254 or 313 nm follows first-order kinetics. The photolysis-rate constants (k_p) were obtained from plots of the first-order decays of the neonicotinoids as a function of time, measured using ATR-FTIR and the absorption bands in the 1590−1620 cm^{-1} region, which were due to asymmetric stretching of $-NO_2$ groups in the nitroguanidines, or the bands in the 2170−2185 cm^{-1} region, which were due to the CN groups in ACM and TCD (Figure 4). The photolysis quantum yields were then calculated from the measured rate constants (k_p) for loss of the NN using eq 1:

$$k_p = \phi \sum_\lambda I_{rel}(\lambda)\sigma(\lambda) \times CF \tag{1}$$

where ϕ is the quantum yield, $I_{rel}(\lambda)$ is the relative lamp intensity, $\sigma(\lambda)$ is the UV-absorption cross section (base e) of the NN as a function of wavelength, and CF is the correction factor for converting the relative values to absolute light intensities using 2-NB as an actinometer.[56,57] The UV-absorption cross sections were measured in this study (Figure S1 and Table S1). For the broadband lamp at 313 nm, the reported quantum yields are averages over 290−350 nm.

Table 1 summarizes the average quantum yields for the photolytic loss of NNs on surfaces in this study (see Tables S3 and S4 for individual experiments). For comparison, those from previous studies in this laboratory are also included.[56,57] The measured UV-absorption cross sections and quantum
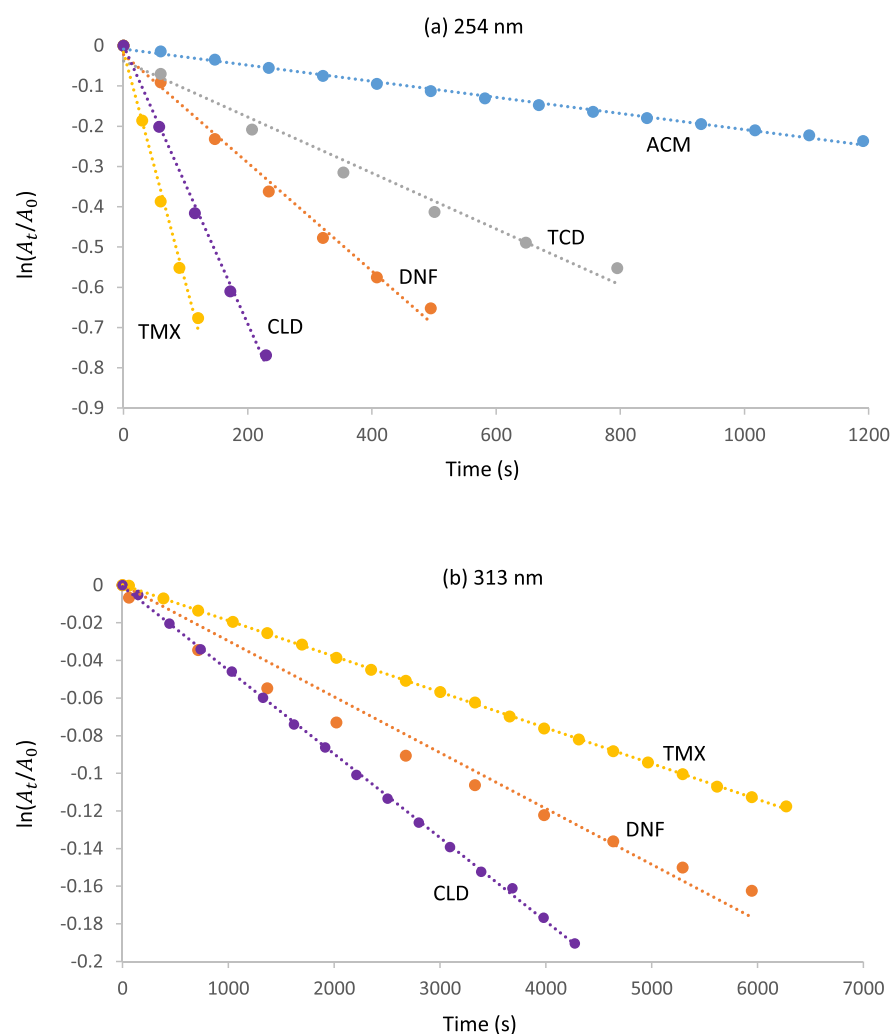
Figure 4. Typical first-order decay of NNs as a function of time. The asymmetric stretching of $-NO_2$ in the $1590-1620$ cm^{-1} region was used for CLD, DNF, and TMX, and the $-CN$-stretching band around 2180 cm^{-1} was used for ACM and TCD. The photolysis-rate constants were obtained from the slopes of the plots.

Table 1. Quantum Yields (ϕ) for Photolysis of Neonicotinoids at Different Wavelengths

NN	photolysis wavelength	condition	ϕ ($\times 10^{-3}$)[a]	reference
IMD	254 nm lamp	ATR crystal	8.5 ± 2.1	Aregahegn et al.[56]
	313 nm lamp	ATR crystal	1.6 ± 0.6	Aregahegn et al.[56]
	270 nm	bidistilled water	0.86 ± 0.17	Redlich et al.[50]
	290−360 nm	borate buffer solution	9.2 ± 0.5	Lu et al.[49]
	300 nm	borate buffer solution	15.1	von Gunten[52]
	natural sunlight	borate buffer solution	5.5	von Gunten[52]
	xenon or natural sun	ultrapure or natural water	10.5 ± 0.2	Todey et al.[51]
CLD	254 nm lamp	ATR crystal	8.0 ± 2.0	this work
	313 nm lamp	ATR crystal	2.2 ± 0.9	this work
	290−360 nm	borate buffer solution	13 ± 1	Lu et al.[49]
	300 nm	borate buffer solution	19.2	von Gunten[52]
	natural sunlight	borate buffer solution	7.3	von Gunten[52]
	xenon or natural sun	ultrapure or natural water	10.1 ± 0.1	Todey et al.[51]
TMX	254 nm lamp	ATR crystal	20 ± 2	this work
	313 nm lamp	ATR crystal	3.9 ± 0.3	this work
	290−360 nm	borate buffer solution	19 ± 1	Lu et al.[49]
	xenon or natural sun	ultrapure or natural water	14 ± 0.2	Todey et al.[51]
DNF	254 nm lamp	ATR crystal	8.6 ± 2.3	this work
	313 nm lamp	ATR crystal	3.3 ± 0.5	this work
ACM	254 nm lamp	ATR crystal	0.75 ± 0.30	this work
	290−360 nm	borate buffer solution	2.2 ± 0.3	Lu et al.[49]

Table 1. continued

NN	photolysis wavelength	condition	ϕ ($\times 10^{-3}$)[a]	reference
	300 nm	borate buffer solution	33.9	von Gunten[52]
TCD	254 nm lamp	ATR crystal	2.1 ± 1.1	this work
	290−360 nm	borate buffer solution	1.3 ± 0.2	Lu et al.[49]
	300 nm	borate buffer solution	46	von Gunten[52]
NPM	254 nm lamp	ATR crystal	12 ± 4	Aregahegn et al.[57]
	313 nm lamp	ATR crystal	1.0 ± 0.3	Aregahegn et al.[57]
	350 nm lamp	ATR crystal	0.94 ± 0.15	Aregahegn et al.[57]
	xenon or natural sun	ultrapure or natural water	24 ± 1	Todey et al.[51]
	254 nm	ultrapure/natural water	39 − 50	González-Mariño et al.[62]
	natural sunlight	ultrapure/natural water	44 − 53	González-Mariño et al.[62]

[a]Errors are ±1s. Quantum yield is defined as the rate of loss of the NN divided by the rate of absorption of photons. Each entry should be multiplied by 10^{-3}, e.g., the first quantum yield is $(8.5 ± 2.1) \times 10^{-3}$.
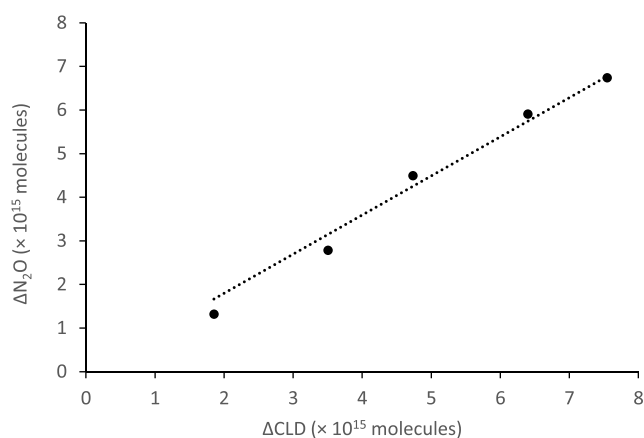

Figure 5. Typical plot of number of molecules of N_2O produced versus number of molecules of CLD reacted during photolysis, obtained by following the 1614 cm^{-1} band.
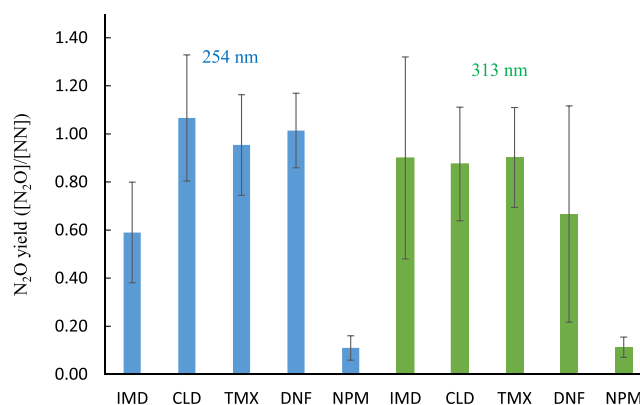

Figure 6. Comparisons of average of N_2O yields from the photolysis of thin films of neonicotinoids in air at 254 nm and with broadband radiation centered at 313 nm as averages in air and N_2. Error bars are 2σ.

yields can be combined with known solar fluxes calculated by Madronich[59] to estimate lifetimes of NNs on solid surfaces in the troposphere. For a solar zenith angle of 35°, corresponding to a location at 40° N latitude on April 1 at noon, the lifetimes of IMD, CLD, TMX, and DNF are estimated to be 16,[56] 15, 10, and 11 h, respectively. For a solar zenith angle of 15°, corresponding to a location at 20° N latitude on April 1 at

noon, the lifetimes of IMD, CLD, TMX, and DNF are estimated to be 13,[56] 12, 8, and 10 h, respectively.

Table 1 also reports the quantum yields for photolysis in aqueous solutions reported by Redlich et al.,[50] Lu et al.,[49] von Gunten,[52] and Todey et al.[51] For similar wavelength regions, the quantum yields for NNs on surfaces are typically smaller than those reported for aqueous solutions. This is not surprising,

Table 2. Nitrous Oxide Yields ($\Delta[N_2O]/\Delta[NN]$) from Photolysis of Thin Films of NN at Different Wavelengths[a]

| NN	photolysis wavelength (nm)	method	vacuum	N_2	air
IMD	254	transmission	0.54 ± 0.22	0.67 ± 0.12	0.65 ± 0.04
		ATR			0.53 ± 0.20[56]
	313	transmission	0.85 ± 0.30	0.88 ± 0.23	0.98 ± 0.10
		ATR			0.88 ± 0.52[56]
CLD	254	transmission	0.59 ± 0.32	0.96 ± 0.14	1.14 ± 0.20
	313	transmission	0.91 ± 0.18	0.89 ± 0.26	0.87 ± 0.16
TMX	254	transmission	0.39 ± 0.12	1.03 ± 0.10	1.02 ± 0.12
		ATR	0.49 ± 0.08	0.88 ± 0.16	0.84 ± 0.10
	313	transmission	0.98 ± 0.16	1.00 ± 0.10	0.95 ± 0.02
		ATR	0.83 ± 0.14	0.91 ± 0.32	0.77 ± 0.16
DNF	254	transmission	0.71 ± 0.22	0.96 ± 0.14	1.00 ± 0.14
		ATR	0.74 ± 0.14	1.00 ± 0.12	1.03 ± 0.22
	313	transmission	0.53 ± 0.16	0.57 ± 0.38	0.54 ± 0.32
		ATR	0.71 ± 0.14	0.94 ± 0.40	0.72 ± 0.12
NPM	254	transmission	0.10 ± 0.02	0.10 ± 0.07	0.11 ± 0.06
		ATR	0.12 ± 0.05	0.11 ± 0.04	0.12 ± 0.04[57]
	313	ATR	0.10 ± 0.01	0.13 ± 0.02	0.10 ± 0.03[57]

[a]Errors are ±2s.
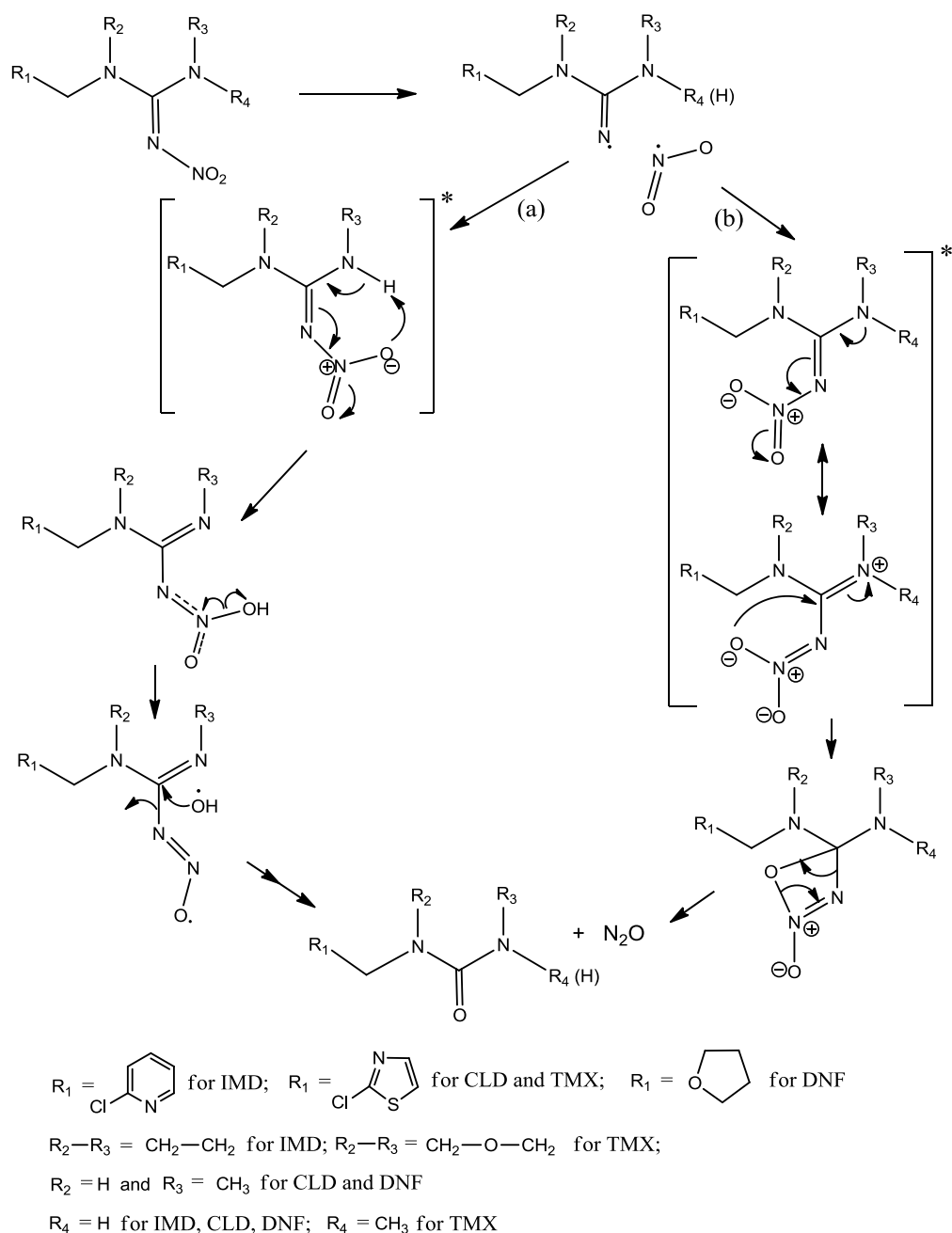
Figure 7. Proposed N$_2$O-formation mechanisms. Pathway a was proposed in a previous study by Aregahegn et al.[56]

because the cage effect is more important in a solid, as in the present studies, than in a lower-viscosity, dynamic solution. Encapsulating the initially formed fragments in this high-viscosity and immobile solid phase greatly enhances their recombination, which regenerates the parent molecule, compared with in the liquid.

Yields of N$_2$O. Figure 5 shows typical data for the formation of N$_2$O as a function of the NN reacted for the photolysis of CLD. Yields obtained from the slopes of such plots are summarized in Table 2 which also includes those from the ATR-FTIR experiments (see Table S5 for individual experiments). Figure 6 compares the average N$_2$O yields for combined air and N$_2$ experiments for each compound for photolysis at 254 or 313 nm. The error bars for the 254 and 313 nm data for an individual compound overlap, suggesting that any differences between the yields at two wavelengths are small. As discussed

in the Experimental Procedures section, the largest factor contributing to the variability in the transmission experiments is the determination of the absolute number of NN reacted based on measurements of a portion of the film. For ATR-FTIR, this is based on only one data point per experiment. In any event, results from the two approaches are in good agreement and show that the N$_2$O yields from the photolysis of nitroguanidines are large.

A previous study[56] of the photolysis of imidacloprid proposed cleavage of −NO$_2$ from IMD as the first step upon UV irradiation. The NO$_2$ and the nitrogen-centered organic radical generated simultaneously then recombine as a result of the "cage effect" in the solid. The energy released during bond formation is sufficient to induce an intramolecular rearrangement in which an OH radical is formed by hydrogen abstraction from the N−H group in the five-membered ring. Held in

the cage, OH is added back to the carbon on the five-membered ring, resulting in ejection of N_2O (Figure 7, path a).[56] The efficiency of this cage effect depends on the initially generated fragments being held in close proximity to enhance their recombination and the formation of N_2O. The other nitroguanidines are expected to react in a similar way, except for TMX, for which the adjacent nitrogen has a $-CH_3$ group rather than an abstractable hydrogen. However, the N_2O yield for TMX is still large at 1 atm pressure in both nitrogen and air (Table 2). We propose here an alternate intramolecular rearrangement after the NO_2 recombination event (Figure 7, path b). The oxygen could attack the carbon in the nitroguanidine moiety, forming a four-membered ring. To eliminate ring strain, the ring undergoes a reverse [2 + 2] cycloaddition to release N_2O.

The quantum yields for nitroguanidines at 254 nm are larger than those at 313 nm. This is likely due to the different electronic excited states involved, resulting in different photochemical-decomposition efficiencies. Given the experimental uncertainties, the N_2O yields are similar at the two wavelengths, suggesting that the same photolysis mechanism applies. However, N_2O yields are smaller under vacuum than in N_2 or air at 254 nm, except for that of NPM, for which the N_2O yield is always small. At the high energy 254 nm radiation, NO_2 may more readily be ejected from the solid phase under vacuum, where diffusion into the gas phase is not limited by higher gas-phase pressures, thus limiting recombination to form N_2O (Figure 7, path a).

The studies reported here used authentic, pure samples of the NN. However, these are applied in the field as formulated materials containing various adjuvants and surfactants so that the NN molecules are in close proximity to other non-NN species. As long as they are in the solid phase, the cage effect that holds the $-NO_2$ and the organic fragment formed upon photolysis should be similar and give similar results. The fact that the N_2O yields are the same in air versus in nitrogen suggests that these fragments recombine sufficiently fast so that secondary reactions of the organic fragment with O_2 do not occur. Nitrous oxide is sufficiently unreactive that if it is formed in the pores of soil particles or close to the surface of a leaf, for example, it should be readily released.

The cyano-containing NN's, ACM and TCD, only absorb UV below 280 nm. Photolysis experiments using the 254 nm lamp were also performed for these two cyanoamidines. As expected, N_2O was not observed as a product from their photolysis because they do not have an $-NO_2$ group.

The formation of N_2O could contribute to the global burden of this greenhouse gas.[61] The annual global production of imidacloprid was estimated to be 20 000 tons in 2010.[2] In 2009, the global neonicotinoid market had grown to US$2.63 billion.[2] On the basis of the market-sales data for individual NNs in 2009[4] and in 2012 for TMX,[2] the annual production of other NNs was estimated relative to the sales of imidacloprid. Production was estimated to be 8000 tons for CLD, 20 000 tons for TMX, 1400 tons for DNF, and 150 tons for NPM. Assuming all of the neonicotinoids were applied and photolyzed with the N_2O yields in this study, the annual production of N_2O from the photolysis of neonicotinoids will be 4.9 Gg of nitrogen per year. This is a small percentage of the total annual anthropogenic N_2O emission of 6.5 Tg of N per year.[61] In addition, even this will be an overestimate because some of the NN will become buried in soils or transferred to groundwater, for example, where sunlight does not penetrate. However, it could have specific-site effects in areas of heavy neonicotinoid use.

■ ASSOCIATED CONTENT

Ⓢ Supporting Information

The Supporting Information is available free of charge on the ACS Publications website at DOI: 10.1021/acs.jafc.8b05417.

> Relative intensity of 313 nm lamp and UV−vis absorption spectra of neonicotinoids in the actinic region; description and schematic of the ATR-FTIR reaction cell; UV-absorption cross sections for nitroguanidines at 313 nm; FTIR-absorption cross sections for nitroguanidines and NPM; photolysis-rate constants and quantum yields for TMX, DNF, ACM, TCD, and CLD on a Ge ATR crystal using different photolysis lamps; and nitrous oxide yields for photolysis of the nitroguanidines and NPM using two different systems at different wavelengths (PDF)

■ AUTHOR INFORMATION

Corresponding Author

*E-mail: bjfinlay@uci.edu. Tel.: (949) 824-7670.

ORCID Ⓘ

Ole John Nielsen: 0000-0002-0088-3937

Barbara J. Finlayson-Pitts: 0000-0003-4650-168X

■ ACKNOWLEDGMENTS

■ REFERENCES

(1) Elbert, A.; Haas, M.; Springer, B.; Thielert, W.; Nauen, R. Applied aspects of neonicotinoid uses in crop protection. *Pest Manage. Sci.* **2008**, *64* (11), 1099−1105.

(2) Simon-Delso, N.; Amaral-Rogers, V.; Belzunces, L. P.; Bonmatin, J. M.; Chagnon, M.; Downs, C.; Furlan, L.; Gibbons, D. W.; Giorio, C.; Girolami, V.; Goulson, D.; Kreutzweiser, D. P.; Krupke, C. H.; Liess, M.; Long, E.; McField, M.; Mineau, P.; Mitchell, E. A. D.; Morrissey, C. A.; Noome, D. A.; Pisa, L.; Settele, J.; Stark, J. D.; Tapparo, A.; Van Dyck, H.; Van Praagh, J.; Van der Sluijs, J. P.; Whitehorn, P. R.; Wiemers, M. Systemic insecticides (neonicotinoids and fipronil): trends, uses, mode of action and metabolites. *Environ. Sci. Pollut. Res.* **2015**, *22* (1), 5−34.

(3) Douglas, M. R.; Tooker, J. F. Large-Scale Deployment of Seed Treatments Has Driven Rapid Increase in Use of Neonicotinoid Insecticides and Preemptive Pest Management in U.S. Field Crops. *Environ. Sci. Technol.* **2015**, *49* (8), 5088−5097.

(4) Jeschke, P.; Nauen, R.; Schindler, M.; Elbert, A. Overview of the status and global strategy for neonicotinoids. *J. Agric. Food Chem.* **2011**, *59* (7), 2897−2908.

(5) Tomizawa, M.; Casida, J. E. Selective toxicity of neonicotinoids attributable to specificity of insect and mammalian nicotinic receptors. *Annu. Rev. Entomol.* **2003**, *48*, 339−364.

(6) Tomizawa, M.; Casida, J. E. Neonicotinoid insecticide toxicology: mechanisms of selective action. *Annu. Rev. Pharmacol. Toxicol.* **2005**, *45* (1), 247−268.

(7) Casida, J. E. Neonicotinoid metabolism: Compounds, substituents, pathways, enzymes, organisms, and relevance. *J. Agric. Food Chem.* 2011, 59 (7), 2923−2931.

(8) *Imidacloprid — risk characterization document: dietary and drinking water exposure*; California Environmental Protection Agency, Department of Pesticide Regulation, 2006.

(9) Matsuda, K.; Kanaoka, S.; Akamatsu, M.; Sattelle, D. B. Diverse actions and target-site selectivity of neonicotinoids: structural insights. *Mol. Pharmacol.* 2009, 76 (1), 1−10.

(10) Wood, T. J.; Goulson, D. The environmental risks of neonicotinoid pesticides: a review of the evidence post 2013. *Environ. Sci. Pollut. Res.* 2017, 24 (21), 17285−17325.

(11) *Pesticide Data Program: Annual Summary, Calendar Year 2015*; USDA, 2016. https://www.ams.usda.gov/press-release/usda-releases-2015-annual-pesticide-data-program-summary (accessed Sept 2017).

(12) Hallmann, C. A.; Foppen, R. P. B.; van Turnhout, C. A. M.; de Kroon, H.; Jongejans, E. Declines in insectivorous birds are associated with high neonicotinoid concentrations. *Nature* 2014, 511, 341−343.

(13) Millot, F.; Decors, A.; Mastain, O.; Quintaine, T.; Berny, P.; Vey, D.; Lasseur, R.; Bro, E. Field evidence of bird poisonings by imidacloprid-treated seeds: a review of incidents reported by the French SAGIR network from 1995 to 2014. *Environ. Sci. Pollut. Res.* 2017, 24 (6), 5469−5485.

(14) Forrester, M. Neonicotinoid insecticide exposures reported to six poison centers in Texas. *Hum. Exp. Toxicol.* 2014, 33 (6), 568−573.

(15) Cimino, A. M.; Boyles, A. L.; Thayer, K. A.; Perry, M. J. Effects of neonicotinoid pesticide exposure on human health: A systematic review. *Environ. Health Perspect.* 2017, 125 (2), 155−162.

(16) Han, W. C.; Tian, Y.; Shen, X. M. Human exposure to neonicotinoid insecticides and the evaluation of their potential toxicity: An overview. *Chemosphere* 2018, 192, 59−65.

(17) Di Prisco, G.; Iannaccone, M.; Ianniello, F.; Ferrara, R.; Caprio, E.; Pennacchio, F.; Capparelli, R. The neonicotinoid insecticide Clothianidin adversely affects immune signaling in a human cell line. *Sci. Rep.* 2017, 7, No. 13446.

(18) Osaka, A.; Ueyama, J.; Kondo, T.; Nomura, H.; Sugiura, Y.; Saito, I.; Nakane, K.; Takaishi, A.; Ogi, H.; Wakusawa, S.; Ito, Y.; Kamijima, M. Exposure characterization of three major insecticide lines in urine of young children in Japan—neonicotinoids, organophosphates, and pyrethroids. *Environ. Res.* 2016, 147, 89−96.

(19) Chang, C. H.; MacIntosh, D.; Lemos, B.; Zhang, Q.; Lu, C. Characterization of daily dietary intake and the health risk of neonicotinoid insecticides for the U.S. population. *J. Agric. Food Chem.* 2018, 66, 10097−10105.

(20) Gibbons, D.; Morrissey, C.; Mineau, P. A review of the direct and indirect effects of neonicotinoids and fipronil on vertebrate wildlife. *Environ. Sci. Pollut. Res.* 2015, 22 (1), 103−118.

(21) van der Sluijs, J. P.; Amaral-Rogers, V.; Belzunces, L. P.; Bijleveld van Lexmond, M. F. I. J.; Bonmatin, J.-M.; Chagnon, M.; Downs, C. A.; Furlan, L.; Gibbons, D. W.; Giorio, C.; Girolami, V.; Goulson, D.; Kreutzweiser, D. P.; Krupke, C.; Liess, M.; Long, E.; McField, M.; Mineau, P.; Mitchell, E. A. D.; Morrissey, C. A.; Noome, D. A.; Pisa, L.; Settele, J.; Simon-Delso, N.; Stark, J. D.; Tapparo, A.; Van Dyck, H.; van Praagh, J.; Whitehorn, P. R.; Wiemers, M. Conclusions of the Worldwide Integrated Assessment on the risks of neonicotinoids and fipronil to biodiversity and ecosystem functioning. *Environ. Sci. Pollut. Res.* 2015, 22 (1), 148−154.

(22) Crossthwaite, A. J.; Bigot, A.; Camblin, P.; Goodchild, J.; Lind, R. J.; Slater, R.; Maienfisch, P. The invertebrate pharmacology of insecticides acting at nicotinic acetylcholine receptors. *J. Pestic. Sci.* 2017, 42 (3−4), 67−83.

(23) Morrissey, C. A.; Mineau, P.; Devries, J. H.; Sanchez-Bayo, F.; Liess, M.; Cavallaro, M. C.; Liber, K. Neonicotinoid contamination of global surface waters and associated risk to aquatic invertebrates: A review. *Environ. Int.* 2015, 74, 291−303.

(24) Rundlof, M.; Andersson, G. K. S.; Bommarco, R.; Fries, I.; Hederstrom, V.; Herbertsson, L.; Jonsson, O.; Klatt, B. K.; Pedersen, T. R.; Yourstone, J.; Smith, H. G. Seed coating with a neonicotinoid

(25) Kessler, S. C.; Tiedeken, E. J.; Simcock, K. L.; Derveau, S.; Mitchell, J.; Softley, S.; Radcliffe, A.; Stout, J. C.; Wright, G. A. Bees prefer foods containing neonicotinoid pesticides. *Nature* 2015, 521 (7550), 74−76.

(26) Raine, N. E.; Gill, R. J. Ecology: Tasteless pesticides affect bees in the field. *Nature* 2015, 521 (7550), 38−40.

(27) Goulson, D.; Nicholls, E.; Botías, C.; Rotheray, E. L. Bee declines driven by combined stress from parasites, pesticides, and lack of flowers. *Science* 2015, 347 (6229), 1255957.

(28) Alkassab, A. T.; Kirchner, W. H. Sublethal exposure to neonicotinoids and related side effects on insect pollinators: honeybees, bumblebees, and solitary bees. *J. Plant Dis. Prot.* 2017, 124 (1), 1−30.

(29) Klein, S.; Cabirol, A.; Devaud, J. M.; Barron, A. B.; Lihoreau, M. Why bees are so vulnerable to environmental stressors. *Trends Ecol. Evol.* 2017, 32 (4), 268−278.

(30) LaLone, C. A.; Villeneuve, D. L.; Wu-Smart, J.; Milsk, R. Y.; Sappington, K.; Garber, K. V.; Housenger, J.; Ankley, G. T. Weight of evidence evaluation of a network of adverse outcome pathways linking activation of the nicotinic acetylcholine receptor in honey bees to colony death. *Sci. Total Environ.* 2017, 584, 751−775.

(31) Brandt, A.; Gorenflo, A.; Siede, R.; Meixner, M.; Buchler, R. The neonicotinoids thiacloprid, imidacloprid, and clothianidin affect the immunocompetence of honey bees (Apis mellifera L.). *J. Insect Physiol.* 2016, 86, 40−47.

(32) Codling, G.; Al Naggar, Y.; Giesy, J. P.; Robertson, A. J. Neonicotinoid insecticides in pollen, honey and adult bees in colonies of the European honey bee (Apis mellifera L.) in Egypt. *Ecotoxicology* 2018, 27 (2), 122−131.

(33) Fairbrother, A.; Purdy, J.; Anderson, T.; Fell, R. Risks of neonicotinoid insecticides to honeybees. *Environ. Toxicol. Chem.* 2014, 33 (4), 719−731.

(34) Forfert, N.; Troxler, A.; Retschnig, G.; Gauthier, L.; Straub, L.; Moritz, R. F. A.; Neumann, P.; Williams, G. R. Neonicotinoid pesticides can reduce honeybee colony genetic diversity. *PLoS One* 2017, 12 (10), e0186109.

(35) Friol, P. S.; Catae, A. F.; Tavares, D. A.; Malaspina, O.; Roat, T. C. Can the exposure of Apis mellifera (Hymenoptera, Apiadae) larvae to a field concentration of thiamethoxam affect newly emerged bees? *Chemosphere* 2017, 185, 56−66.

(36) Tavares, D. A.; Dussaubat, C.; Kretzschmar, A.; Carvalho, S. M.; Silva-Zacarin, E. C. M.; Malaspina, O.; Berail, G.; Brunet, J. L.; Belzunces, L. P. Exposure of larvae to thiamethoxam affects the survival and physiology of the honey bee at post-embryonic stages. *Environ. Pollut.* 2017, 229, 386−393.

(37) Tosi, S.; Burgio, G.; Nieh, J. C. A common neonicotinoid pesticide, thiamethoxam, impairs honey bee flight ability. *Sci. Rep.* 2017, 7, 1201.

(38) Tosi, S.; Nieh, J. C. A common neonicotinoid pesticide, thiamethoxam, alters honey bee activity, motor functions, and movement to light. *Sci. Rep.* 2017, 7, 15132.

(39) Tosi, S.; Nieh, J. C.; Sgolastra, F.; Cabbri, R.; Medrzycki, P. Neonicotinoid pesticides and nutritional stress synergistically reduce survival in honey bees. *Proc. R. Soc. London, Ser. B* 2017, 284 (1869), 20171711.

(40) Wu, M. C.; Chang, Y. W.; Lu, K. H.; Yang, E. C. Gene expression changes in honey bees induced by sublethal imidacloprid exposure during the larval stage. *Insect Biochem. Mol. Biol.* 2017, 88, 12−20.

(41) Mitchell, E. A. D.; Mulhauser, B.; Mulot, M.; Mutabazi, A.; Glauser, G.; Aebi, A. A worldwide survey of neonicotinoids in honey. *Science* 2017, 358, 109−111.

(42) Solomon, K. R.; Stephenson, G. L. Quantitative weight of evidence assessment of higher-tier studies on the toxicity and risks of neonicotinoid insecticides in honeybees 1: Methods. *J. Toxicol. Environ. Health, Part B* 2017, 20 (6−7), 316−329.

insecticide negatively affects wild bees. *Nature* 2015, 521 (7550), 77−80.

(43) Solomon, K. R.; Stephenson, G. L. Quantitative weight of evidence assessment of higher tier studies on the toxicity and risks of neonicotinoids in honeybees. 3. Clothianidin. *J. Toxicol. Environ. Health, Part B* **2017**, *20* (6−7), 346−364.

(44) Sponsler, D. B.; Johnson, R. M. Mechanistic modeling of pesticide exposure: The missing keystone of honey bee toxicology. *Environ. Toxicol. Chem.* **2017**, *36* (4), 871−881.

(45) Stephenson, G. L.; Solomon, K. R. Quantitative weight of evidence assessment of higher-tier studies on the toxicity and risks of neonicotinoids in honeybees. 2. Imidacloprid. *J. Toxicol. Environ. Health, Part B* **2017**, *20* (6−7), 330−345.

(46) Tsvetkov, N.; Samson-Robert, O.; Sood, K.; Patel, H. S.; Malena, D. A.; Gajiwala, P. H.; Maciukiewicz, P.; Fournier, V.; Zayed, A. Chronic exposure to neonicotinoids reduces honey bee health near corn crops. *Science* **2017**, *356* (6345), 1395−1397.

(47) Stephenson, G. L.; Solomon, K. R. Quantitative weight of evidence assessment of higher tier studies on the toxicity and risks of neonicotinoids in honeybees. 4. Thiamethoxam. *J. Toxicol. Environ. Health, Part B* **2017**, *20* (6−7), 365−382.

(48) Bonmatin, J. M.; Giorio, C.; Girolami, V.; Goulson, D.; Kreutzweiser, D. P.; Krupke, C.; Liess, M.; Long, E.; Marzaro, M.; Mitchell, E. A. D.; Noome, D. A.; Simon-Delso, N.; Tapparo, A. Environmental fate and exposure; neonicotinoids and fipronil. *Environ. Sci. Pollut. Res.* **2015**, *22* (1), 35−67.

(49) Lu, Z.; Challis, J. K.; Wong, C. S. Quantum yields for direct photolysis of neonicotinoid insecticides in water: implications for exposure to nontarget aquatic organisms. *Environ. Sci. Technol. Lett.* **2015**, *2* (7), 188−192.

(50) Redlich, D.; Shahin, N.; Ekici, P.; Friess, A.; Parlar, H. Kinetical study of the photoinduced degradation of imidacloprid in aquatic media. *Clean: Soil, Air, Water* **2007**, *35* (5), 452−458.

(51) Todey, S. A.; Fallon, A. M.; Arnold, W. A. Neonicotinoid insecticide hydrolysis and photolysis: Rate and redisual toxicity. *Environ. Toxicol. Chem.* **2018**, *37*, 2797.

(52) von Gunten, K. Photodegradation and sorption to Na-SAz clay, soil, and pollen of the neonicotinoids acetamiprid, clothianidin, imidacloprid and thiacloprid. BS Thesis, ETH Zurich, Zurich, Switzerland, 2012.

(53) Scholz, K.; Reinhard, F. Photolysis of imidacloprid (NTN 33893) on the leaf surface of tomato plants. *Pestic. Sci.* **1999**, *55* (6), 652−654.

(54) Schippers, N.; Schwack, W. Phototransformation of imidacloprid on isolated tomato fruit cuticles and on tomato fruits. *J. Photochem. Photobiol., B* **2010**, *98* (1), 57−60.

(55) Schippers, N.; Schwack, W. Photochemistry of imidacloprid in model systems. *J. Agric. Food Chem.* **2008**, *56* (17), 8023−8029.

(56) Aregahegn, K. Z.; Shemesh, D.; Gerber, R. B.; Finlayson-Pitts, B. J. Photochemistry of thin solid films of the neonicotinoid imidacloprid on surfaces. *Environ. Sci. Technol.* **2017**, *51* (5), 2660−2668.

(57) Aregahegn, K. Z.; Ezell, M. J.; Finlayson-Pitts, B. J. Photochemistry of solid films of the neonicotinoid nitenpyram. *Environ. Sci. Technol.* **2018**, *52* (5), 2760−2767.

(58) *Climate Change 2013: The Physical Science Basis*; Contribution of Working Group I to the Fifth Assessment Report of the Intergovernmental Panel on Climate Change; IPCC, 2013.

(59) Finlayson-Pitts, B. J.; Pitts, J. N. *Chemistry of the Upper and Lower Atmosphere: Theory, Experiments, and Applications*; Academic Press: San Diego, 2000.

(60) Socrates, G. *Infrared and Raman characteristic group frequencies: tables and charts*, 3rd ed.; Wiley: New York, 2004.

(61) Tian, H. Q.; Lu, C. Q.; Ciais, P.; Michalak, A. M.; Canadell, J. G.; Saikawa, E.; Huntzinger, D. N.; Gurney, K. R.; Sitch, S.; Zhang, B. W.; Yang, J.; Bousquet, P.; Bruhwiler, L.; Chen, G. S.; Dlugokencky, E.; Friedlingstein, P.; Melillo, J.; Pan, S. F.; Poulter, B.; Prinn, R.; Saunois, M.; Schwalm, C. R.; Wofsy, S. C. The terrestrial biosphere as a net source of greenhouse gases to the atmosphere. *Nature* **2016**, *531* (7593), 225−232.

(62) González-Mariño, I; Rodríguez, I.; Rojo, L.; Cela, R. Photodegradation of nitenpyram under UV and solar radiation: Kinetics, transformation products identification and toxicity predictions. *Sci. Tot. Environ.* **2018**, *644*, 995−1005.